ELSEVIER

Journal of Molecular Catalysis A: Chemical 143 (1999) 71–83

JOURNAL OF MOLECULAR CATALYSIS A: CHEMICAL

www.elsevier.com/locate/molcata

The mechanism of the phosphine-modified nickel-catalyzed acetic acid process

William R. Moser [a,*], Barbara J. Marshik-Guerts [a], Stanley J. Okrasinski [b]

[a] *Department of Chemical Engineering, Worcester Polytechnic Institute, Worcester, MA 01609, USA*
[b] *Eastman Chemical, Kingsport, TN 37662, USA*

Received 26 May 1998; accepted 15 July 1998

Abstract

The nickel-catalyzed methanol (MeOH) carbonylation reaction was studied with an in situ infrared technique using a high pressure cylindrical internal reflectance reactor (CIR-reactor). The role of phosphine ligands was investigated in order to determine the relationship between the structural and electronic properties of the ligand and catalytic properties. It was found that the highest carbonylation rates occurred for the phosphine ligands having the greatest cone angles. Altering the electronic properties of substituted triarylphosphines resulted in systematic changes in the carbonylation rate, and a Hammett treatment of the rate data using normal sigma constants led to a volcano plot. A modified Hammett plot using Taft polar sigma constants for various trialkylphosphines led to a linear relationship in which the rate increased as the electron-donating properties of the ligand increased. The carbonylation activity was correlated with the steric size of trialkylphosphines by the observation of a linear relationship to the ligands cone angle. The in situ reaction monitoring studies showed that the phosphine ligand was substantially converted to the corresponding phosphonium salt through reaction with excess methyl iodide in the system. The in situ reaction monitoring studies, conducted at typical process conditions, showed that the phosphonium salt reversibly dissociated to differing amounts of the free phosphine depending on the electronic and steric properties of the phosphine. The reaction monitoring studies, using phosphines of widely differing electronic and steric properties showed that the reaction rates increased linearly as the concentration of free PR_3 in solution increased. The results of this ligand study and a prior process parameter study led to a reaction mechanism in which phosphine is mainly transformed to $[P(CH_3)R_3]^+I^-$. It was shown that this soluble salt partially dissociates to provide sufficient free phosphine to coordinate to Ni° to form the active catalyst. A low partial pressure of hydrogen was found essential to provide the catalytic cycle with reduced nickel. The Ni° combines with free PR_3, forming $Ni(PR_3)_2$ which is located within the active catalytic cycle. The kinetic data and in situ reaction monitoring observations are consistent with a reversible slow step in the active cycle consisting of CH_3I reacting with $Ni(PR_3)_2$, forming an oxidative addition product which is rapidly carbonylated. All other subsequent steps are much faster than the oxidative addition reaction.

Keywords: Phosphine; Nickel; Acetic acid

* Corresponding author. E-mail: wmoser@wpi.edu

1381-1169/99/$ - see front matter
PII: S1381-1169(98)00369-0

1. Introduction

The rhodium-catalyzed acetic acid (AcOH) process has been used extensively in industry [1–6]. Recent advances in the development of group VIII metal complexes have given rise to promising catalysts for carbonylation reactions at lower temperatures and pressures [7–13]. Our preceding paper investigated the acetic acid process using a phosphine-modified nickel catalyst in a non-aqueous solvent mixture of methyl acetate (MeOAc) and methanol (MeOH) [14]. From a process design point of view, a more feasible route to AcOH would be to use a co-solvent system consisting of both the reactant and the desired product, i.e., MeOH and AcOH, which simplified product separation. Therefore, the process parameters in this study were optimized to provide both high reaction rates and yields of AcOH, using an AcOH/MeOH co-solvent mixture. In order to run the reaction in a highly acidic medium such as water-acetic acid-iodide, a Hastelloy C reactor was used to avoid corrosion.

The mechanism of the Ni-based acetic acid process was previously proposed to be similar to the Rh-based system. One of the important intermediates within the active catalytic cycle was proposed to be $[NiI(CO)_3]^-$ [9–13]. In a prior paper [14], we examined the nickel-catalyzed acetic acid process in a non-aqueous, MeOH–MeOAc system using an in situ technique based on cylindrical internal reflectance-Fourier transform infrared spectroscopy (CIR-FTIR) [15,16]. This study demonstrated that this anionic species was not at all detected under process conditions of high carbonylation rates [14]. Furthermore, none of the $Ni(CO)_xL_y^{n-}$ family of complexes was detected at high reaction rates, other than a trace amount of $Ni(CO)_4$. These species were detected during heat up to reaction conditions where the active catalyst was being formed from NiI_2, PPh_3, CO, and H_2. Through a combination of kinetic results under a variety of process conditions and in situ reaction monitoring using the CIR-reactor technique, a mechanism was suggested for the formation of acetic acid from MeOH and CO based upon the formation of the catalytically active species, $Ni(PPh_3)_2$ [14].

The present study examines the effect of the electronic and steric properties of organophosphine ligands on the aqueous acetic acid system. The kinetic and in situ reaction monitoring data from this study will be combined with the results from the process parameter studies in the prior paper [14] to derive a more complete catalytic mechanism. Previous studies [17,18], as well as our own, demonstrated that phosphines not only stabilize the active catalyst but also have a substantial effect on the carbonylation rate. Thus, alterations in the steric and electronic properties of phosphines were examined to determine their effect on carbonylation rates, product selectivity, and nickel complex speciation under autogenous conditions.

In this study, a series of ligands having differing steric sizes was investigated to determine the effect of the ligand's cone angle on the carbonylation rates and nickel speciation. The electronic effect on catalyst performance was investigated with a series of substituted triaryl phosphines and by analyzing its reaction rates by a variety of Hammett-type treatments. In situ infrared experiments were carried out while the steric and electronic character of the phosphine ligand was varied to determine (a) which phosphine structure gave rise to the highest equilibrium concentrations of free phosphines; and (b) whether the free phosphine concentration was related to the carbonylation rates.

Other factors influencing the mechanistic pathway were also investigated. The induction period was monitored as a function of phosphine structure to gain information on factors controlling the rate of active catalyst formation. Finally, the influence of the phosphine's structures on the concentration of $Ni(CO)_4$ was studied to gain further evidence as to any role the species played in catalysis. A second objective

was to identify process conditions leading to the elimination of all $Ni(CO)_4$ at high rates of AcOH production.

2. Previously proposed mechanisms

In 1986, Dekleva and Forster [6] reviewed the current literature on the nickel-catalyzed acetic acid process and concluded that the evidence for the various mechanisms proposed was insufficient to support claims of the active metal species as either $Ni(CO)_4$ or $[NiI(CO)_3]^-$. The three most important mechanisms for the nickel-catalyzed carbonylation of MeOH to acetic acid will be considered here. The first, by Gauthier-Lafaye and Perron [13] of Rhône-Poulenc, postulated that the reaction mechanism involves a $[NiX(CO)_3]^-$ species from the reaction of:

$$Ni(CO)_4 + X\text{–}A \leftrightarrow A^+[Ni(CO)_3X]^- + CO \quad (1)$$

The $[X]^-$ species was produced from various sources such as alkali iodides or quaternized phosphonium salts, $[A]^+$ being the counter cation. The rate-determining step was postulated as the oxidative addition of MeI to $[NiX(CO)_3]^-$. This was followed by methyl migration with CO insertion, and finally reductive elimination of acetyl iodide, which eventually formed acetic acid upon reaction with water. Their proposed mechanism was based on extensive work performed on the system using *N*-methylpyrrolidinone or acetic acid as the solvent.

The next mechanistic pathway was reported in 1987 by Rizkala [17] of Halcon, and supported much of the Rhône-Poulenc work. Both works proposed that the Ni catalyst was stabilized by either an organo-phosphorus or a organo-nitrogen promoter [13,17]. Unlike the Rhône-Poulenc work or the Rh-based system, Rizkala postulated that the phosphorus promoter was needed to keep the Ni species in solution. Therefore, the active metal species was proposed as a Ni–phosphine complex that originated from $Ni(CO)_4$ by ligand displacement. The active metal species was proposed in two possible forms:

$$Ni(CO)_4 + PR_3 \rightleftharpoons Ni(CO)_3(PR_3) + CO \quad (2)$$

or

$$Ni(CO)_4 + 2PR_3 \leftrightarrow Ni(CO)_2(PR_3)_2 + 2CO \quad (3)$$

The di- or tri-carbonyl phosphine complex then formed a penta-coordinated di-carbonyl Ni species upon oxidative addition of MeI. They proposed that the penta-coordinated species is highly unstable; therefore, a facile CO insertion occurred to form a four-coordinate $[NiI(COCH_3)(CO)(PR_3)]$ species [18].

Since quaternary phosphonium salts form readily in the presence of MeI, Rizkala's claim of an active Ni catalyst, containing phosphorus ligands, was questioned by Dekleva and Forster. Indeed, the Rhône-Poulenc group found no change in the carbonylation rate when using the quaternary salt in place of the original phosphine [13]. No studies were reported to determine the extent of phosphine and phosphonium salt formation under reaction conditions.

The final mechanistic proposal was presented in 1986 by Nelson et al. [12] of Eastman Chemicals. The mechanistic pathway was based upon the results from Eastman and also on the mechanism proposed by Dekleva and Forster [11] of Monsanto for the Ni-based acetic acid reaction. The work by Nelson et al. supported the hypothesis that the active metal species was $[NiI(CO)_3]^-$, originally proposed by Dekleva and Forster, based upon the original work of Reppe et al. [19] patented in 1956 [17]. Reppe proposed that the nickel-based acetic acid process involved the oxidative addition of MeI to $Ni(CO)_4$ [7,19,20].

Nelson et al. used an in situ FTIR reactor run in the transmission mode. The system consisted of a series of transfer lines to and from a high pressure/high temperature reactor. The path-

way could be switched to a high-pressure flow through the FTIR cell. Nelson et al. followed the formation of a peak at 1959 cm^{-1}, which they assigned to $[NiI(CO)_3]^-$. They followed the intensity of the 1959 cm^{-1} peak as the reaction progressed, and reported a linear correlation between the $[Ni(CO)_3]^-$ concentration and an increase in the MeOAc carbonylation rate. Hence, they proposed one of the active species in the cycle to be $[NiI(CO)_3]^-$. While Nelson et al. had originally studied the carbonylation of MeOAc to acetic anhydride, the studies of Zoeller [21] on the acetic acid process using transmission infrared equipment concluded that a similar mechanism was likely for the process. This mechanism is widely accepted as the probable pathway for the nickel catalyzed acetic acid process.

The Eastman study [21] concluded that approximately 10 times as much Ni was needed to obtain high reaction rates as compared to the Rh-based system. It was also found that as the H_2/CO partial pressure was increased, a critical CO pressure was required to form the active catalyst. The rate-determining step was believed to be the oxidative addition of MeI to the $[NiI(CO)_3]^-$ species. The results of the study reported here suggest an alternative mechanism as contrasted to those previously proposed. The difference in the nickel complex speciation in these studies, as contrasted to the transmission cell experiment reported before, is likely due to the fact that the CIR-reactor technique used here measures species concentrations under well-stirred in situ conditions directly within the high-pressure zone of the reactor in real time.

3. Experimental

In all experiments, acetic acid and MeOH were used as co-solvents in a 60:40 volume ratio; 4% v/v H_2O was added to the mixture to eliminate the formation of acetic anhydride. The reaction system used in this study was described in detail elsewhere [15]. The reactor consisted of a PARR high-pressure/high-temperature micro-reactor modified to contain a monocrystalline silicon (Si) rod used for propagating the IR waves throughout the reaction solution. The IR beams are collected via a Bausch and Laumb CIR optical mirror assembly all contained within the chamber of a Nicolet 510P FTIR spectrometer. Out of safety considerations, the entire reaction system and spectrometer were contained within a high-velocity flow hood, and the spectrometer was constantly purged with a high volume of nitrogen.

CH_3OH, CH_3CO_2H, H_2O, LiI, MeI, NiI_2, and PR_3 were added to the micro-reactor, fabricated from Hastalloy C, in a glove box under a dry nitrogen purge. The starting concentrations for all experiments were the same, unless stated otherwise, with the concentration of NiI_2 at 0.18 M, LiI at 0.60 M, and H_2O at 4 wt.%, and all reactions used a solvent consisting of CH_3OH and CH_3CO_2H. The concentrations of the phosphine components varied with the experiment and they are specifically mentioned in Section 4 and expressed as a molar ratio of the amount of Ni initially charged to the reactor.

The reactions were all performed at 160°C with an internal pressure of 8.16 kPa (900 psig), maintained by the constant addition of CO gas. Each infrared spectrum resulted from the averaging of 500 scans of data at 4 cm^{-1} resolution, using a total scan time of approximately 5 min. No smoothing was applied to the displayed spectra. The spectra were then analyzed in the region from 2200 to 1440 cm^{-1}. The carbonylation reaction rates were determined by analyzing the peak areas for acetic acid in the region from 1800 to 1650 cm^{-1}. Steady state rates were calculated at points which were well past the induction time, after the MeOH conversion was about 20%.

4. Results and discussion

Table 1 contains a comprehensive list of the main runs to determine the optimum process

Table 1
Carbonylation reaction rates for (A) MeI/Ni ratio held constant while adding [MeI]; (B) MeI/P ratio constant with increasing [MeI]; (C) P/Ni ratio kept constant as the [MeI] was increased; (D) MeI_{free}/Ni ratio maintained at 5.08 while raising the overall [MeI]

(A) Rate $\times 10^{-4}$ (M/min)	P/Ni	MeI/P	Constant MeI/Ni
1.39	1.00	7.40	7.40
1.92	3.10	2.37	7.36
2.37	3.99	1.85	7.40
2.96	5.06	1.47	7.43
1.45	7.00	1.06	7.41

(B) Rate $\times 10^{-4}$ (M/min)	P/Ni	MeI/Ni	Constant MeI/P
1.72	3.09	4.60	1.49
2.96	5.06	7.43	1.47
2.96	7.00	10.26	1.47
2.35	8.98	13.16	1.47

(C) Rate $\times 10^{-4}$ (M/min)	MeI/Ni	MeI/P	Constant P/Ni
3.12	14.34	4.64	3.09
3.09	9.06	2.92	3.1
2.79	8.18	2.64	3.1
1.92	7.36	2.37	3.1
1.78	5.99	1.93	3.09
1.70	6.01	1.94	3.09
1.69	4.60	1.48	3.1
1.72	4.60	1.49	3.09
0.78	3.00	0.97	3.1

(D) Rate $\times 10^{-4}$ (M/min)	P/Ni	MeI/Ni	MeI/P
1.60	2.00	7.08	3.54
2.79	3.10	8.18	2.64
4.49	4.00	9.07	2.27
3.91	4.50	9.58	2.13
3.75	6.00	11.78	1.96

parameters for obtaining the highest rates of carbonylation of MeOH to acetic acid in the MeOH–acetic acid–water solvent system. The highest reaction rates were observed for the conditions listed in Table 1D. A comparison of the optimum process conditions used to obtain maximum rates for the $AcOH/MeOH/H_2O$ system to the MeOAc/MeOH system is presented in Table 2. These data show that in order for the $AcOH/MeOH/H_2O$ system to proceed at comparable rates to those of the MeOH/MeOAc system, it was necessary to use almost twice the amount of both the phosphorus component and MeI.

4.1. Process optimization for the aqueous MeOH acetic acid system

A variety of process parameters was examined to determine the optimum for the aqueous MeOH–acetic acid solvent system. It was found that the optimum conditions were quite different from those determined using the MeOH–MeOAc system [14]. The results of the optimization study are listed in Table 1. The highest reaction rate of this series was found when there was a constant amount of excess or 'free' MeI in the reaction mixture (Table 1D). The excess amount was calculated from the amount of MeI required for the stoichiometric reaction between CH_3I and PR_3 forming $[(CH_3)PR_3]^+I^-$. Then an additional excess amount of CH_3I was added based on the amount of Ni used in the reaction. The excess amount which was applied in all reactions was 5.08/1.0 of CH_3I/Ni.

The dependency of the reaction rate on the total MeI/Ni ratio, is presented in Table 1B–D and plotted in Fig. 1. This figure shows the reaction rate as a function of the total MeI/Ni ratio. All three sets of data indicate that the rate appears to peak or level-off at a MeI/Ni ratio near 9. In these experiments, using a constant amount of MeI_{free} (Fig. 1,□), the overall reaction rate increased sharply to a maximum near a total MeI/Ni ratio of 9 then decreased and

Table 2
Final process parameters for obtaining the maximum carbonylation rates for the original conditions for both the MeOAc/MeOH and the AcOH/MeOH co-solvent systems

Solvent	P/Ni	MeI/Ni	Ni concentration (M)	Rate $\times 10^{-4}$ (M/min)
MeOAc/MeOH	2.0	4.0	0.18	4.99
AcOH/MeOH	5.0	9.0	0.18	3.67

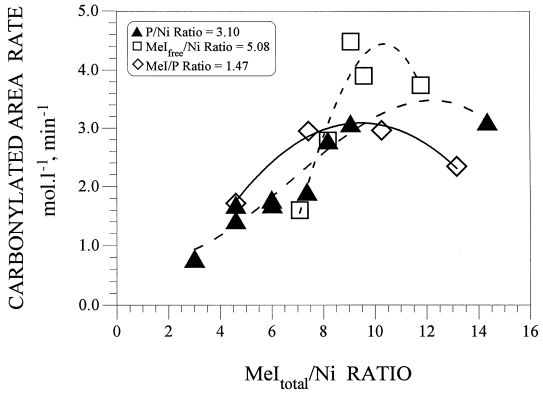

Fig. 1. Graph of the carbonylation rate as a function of the total amount of MeI in the reaction as a function of Ni. Curve (□): an excess of MeI was maintained over the amount of a 1:1 molar ratio of MeI to P in the amount of 5.08 mol of MeI/Ni. (▲) The P/Ni ratio was maximized at 3.10 while changing the [MeI]. (◇) The MeI/P ratio was 1.47 as the [MeI] was increased.

leveled off. Since the carbonylation rates were higher using a constant amount of excess CH_3I, this excess was used in all subsequent experiments.

4.2. Comparison of phosphine to phosphonium salt reactivity

A series of experiments was designed to examine the effect on carbonylation rates when the initially charged phosphorus component was either the free phosphine, or alternatively, the corresponding phosphonium salt. In all cases, a 5.08 molar ratio of CH_3I/Ni was employed in excess of the amount of CH_3I required in theory to convert all free PR_3 to the phosphonium salt.

Fig. 2 and Table 3 show a comparison in the carbonylation activity when PPh_3 and CH_3I were initially charged to the reactor as compared to the reaction where $[P(CH_3)Ph_3]^+I^-$ and CH_3I were initially charged. The figures show that the reaction rate using the free phosphine was 3.67 mol/min which was slightly faster than the one using the phosphonium salt (3.11 mol/min). These results were compared to reactions using $[P(CH_3)_4]^+I^-$ and CH_3I with free $P(CH_3)_3$ and CH_3I. Fig. 2 also shows that the PPh_3 system is more reactive than $P(CH_3)_3$, and both phosphonium salts and $P(CH_3)_3$ are of similar reactivity. The low reactivity of the $P(CH_3)_3$ ligand and its phosphonium salt is likely due to the greater basicity of this ligand compared to PPh_3, resulting in nearly complete conversion of any free $P(CH_3)_3$ ligand to the corresponding phosphonium salt. These data suggest the importance of free phosphine in the reaction mixture, and will be addressed later in this paper. Under conditions of rapid carbonylation, it was shown from the in situ infrared reaction monitoring data that $[P(CH_3)Ph_3]^+I^-$ was 15% dissociated to free PPh_3. A wider study of phosphines, discussed later, showed that the carbonylation rates were dependent on the amount of free phosphine present in the active solutions.

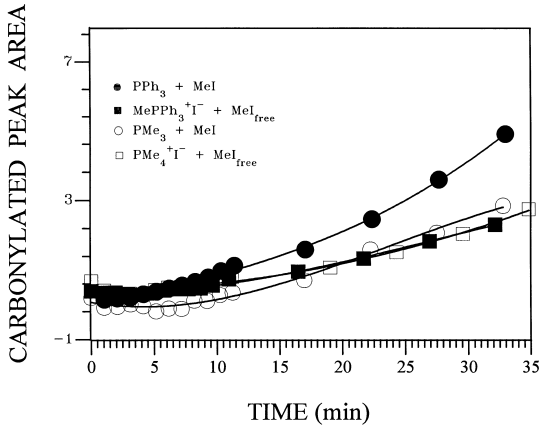

Fig. 2. The reaction rate and the induction period were probed as a function of the type of the phosphine ligand. (A) Plot of the reaction rate as a function of PR_3: PPh_3 (●) and $MePPh_3^+I^-$ (■) vs. PMe_3 (○) and $PMe_4^+I^-$ (□).

Table 3
Determination of the effect of the formation or the dissociation of the quaternary salt upon the carbonylation reaction rate

Reaction	Carbonylation rate $\times 10^{-4}$ (M/min)
$PPh_3 + PhI$	3.47
$PPh_4^+I^- + MeI$	3.36
$PPh_3 + MeI$	3.67
$MePPh_3^+I^- + MeI$	3.11
$PMe_3 + MeI$	2.12
$PMe_4^+I^- + MeI$	2.02
$PPh_3 + PhI + MeI$	3.24

4.3. Effect on carbonylation rates by steric variation of the phosphine ligand

From the results above, it was concluded that the active carbonylation solutions needed to contain some free PPh_3 ligand. To examine this possibility in more detail, two series of experiments were performed with phosphine ligands differing in either their steric size, as measured by the subtended cone angle [22], or in their electronic properties [23] as determined by Hammett-type reactivity using Taft sigma constants. Table 4A lists the carbonylation rate data as a function of alkyl ligand and Table 4B as a function of substituted aryl ligand.

In the case of the alkyl ligands, the steric effects were varied over a wide range of sizes from $P(CH_3)_3$ to $P(t\text{-}Bu_3)_3$. Two possible effects are expected in the comparison of small vs. large ligands. Large ligands such as tertiary-butylphosphine would be expected to form NiL_n complexes of lower coordination numbers such as NiL_2, and the sterically bulky phosphine would also react with CH_3I to a lesser extent, resulting in a high mole fraction of free phosphine in solution and less of the phosphonium salt. The latter effect provides the requisite amount of free phosphine to interact with Ni° in the active catalytic cycle, and the former effect results in a more favorable amount of NiL_2 within the cycle.

Table 4
Comparison of the (A) alkyl vs. (B) phenyl phosphonium ligand to extract information on the effect of the steric or electronic properties, respectively, upon the carbonylation reaction rate

Phosphine ligand	Carbonylation rate $\times 10^{-4}$ (M/min)
(A) Alkyl ligands	
$P(Me)_3$	2.54
$P(n\text{-}Bu)_3$	2.87
$P(Ph)_3$	3.67
$P(i\text{-}Pr)_3$	3.55
$P(Cy)_3$	3.82
$P(t\text{-}Bu)_3$	4.75
(B) Substituted phenyl ligands	
$P(p\text{-}PhOMe)_3$	2.21
$P(p\text{-}PhMe)_3$	2.95
$P(Ph_3)_3$	3.67
$P(m\text{-}PhOMe)_3$	2.66
$P(p\text{-}PhCl)_3$	0.54
$P(p\text{-}PhCF_3)_3$	2.05

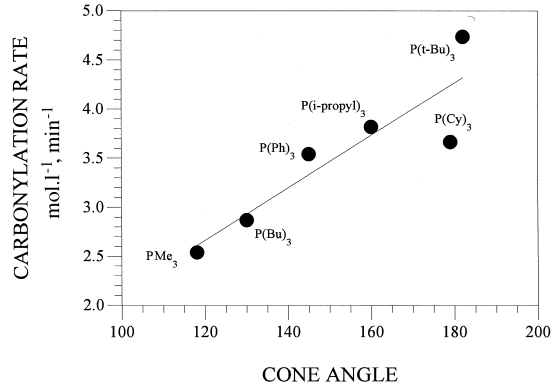

Fig. 3. Steric interference was analyzed by plotting the calculated cone angle of the various alkyl ligands as a function of the reaction rate.

The effect of the steric interaction by the phosphine can be seen in a plot of the carbonylation rate vs. cone angle for the different ligands in Fig. 3. As expected, the ligands with greater steric hindrance resulted in increased carbonylation reaction rates. In general, it was not possible to quantify the amount of free phosphine in the active solutions using these trialkylphosphines since the strong infrared bands for most of the alkyl ligands appeared below the spectral cut-off at 1400 cm^{-1} of the Si crystal used in the CIR-FTIR experiments. The exception to this case was $P(t\text{-}Bu)_3$ which will be discussed in detail in Section 5. Thus, no conclusion could be drawn from the in situ FTIR experiments as to whether the rate increase corresponded to an increase in the amount of free phosphine in the active solutions or not. However, it was apparent that the bulkier ligands resulted in greater carbonylation rates (Fig. 3).

To shed some understanding on whether the rates increased due to purely steric or partially electronic reasons, the catalytic carbonylation rates were examined as a function of the electron availability on the P-atom resulting from sigma electron donation or withdrawing through

the P–alkyl bond. One technique for estimation of electronic effects for alkyls, where there is the potential for significant steric effects, is the two-parameters Taft treatment [24]. In this treatment induction, sigma and steric substituent constants were derived and applied to understand structure rate effects [25] in organic reactions. In the application of this method to trialkyl phosphines shown in Fig. 4, the carbonylation rates are plotted as a function of the Taft sigma* constant [25], a measure of substituent bonding strengths. These polar substituent constants describe the sigma-donating contribution of the alkyl ligands on phosphorus only, but it affects the bonding between the phosphine ligand and the Ni metal as well as the stability of the corresponding phosphonium salts resulting from the reaction of free phosphine and CH_3I. In the figure, the more electron-donating substituents have negative values, and electron-withdrawing, have positive values. The negative slope observed for the reactivity line indicates that electronically donating substituents favor faster rates of carbonylation. The importance of the simultaneously acting steric effects for each ligand is obtained by determining from the statistics of the best-fit linear regression line the intercept at sigma* of 0.0. Then the steric substituent constants (E_s) are applied with the value of the intercept to determine the sensitivity of steric effects that are pertinent to each particular

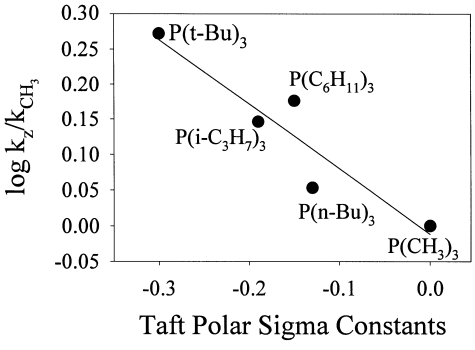

Fig. 4. The strength of the sigma bond between the P and the alkyl ligand is plotted as the carbonylation rate vs. the Taft polar sigma* constants.

substituent. The data in Fig. 4 show that as the electron-donating character of the trialkylphosphines increased (towards more negative sigma* values), the carbonylation rates increased. The ρ^* derived from this treatment was -0.92, indicating a moderate effect of electron donation to accelerate the overall rates of carbonylation. Our interpretation of this data is that when the steric components of the ligand are large such as in P(*t*-butyl)$_3$, the reaction with methyl iodide to remove free phosphine is diminished, but the residual sigma* electron donation of this type of ligand increases the electron density on Ni in the co-ordination complex in the active cycle, NiL_2. This has the effect to facilitate the reaction with methyl iodide to form the product of oxidative addition.

4.4. Effect on carbonylation rates by electronic variation of the phosphine ligand

In order to separate the electronic contributions from steric effects, substituted *para*-triphenylphosphine ligands were used to examine the effects of electronic variations on the carbonylation rate. This study enabled the electronic effects to be isolated from steric effects since there was essentially no difference between the steric hindrance of the *para*-substituted triarylphosphine ligands used in the carbonylation experiments.

The electronic effects were systematically varied by changing the *para*-substituent bound to the aromatic nucleus of the triarylphosphines by electron-withdrawing or electron-donating substituent. The subsequent MeOH carbonylation rates were plotted vs. the normal Hammett sigma constants, resulting in the formation of a volcano-type plot as seen in Fig. 5. The Hammett constant is a measure of the electronic effect caused by substituting various groups on an aromatic ring. A negative value indicates the group is electron-donating. The scale is referenced to *p*-H at 0.0 for a substituent being neither electron-donating or -withdrawing. As

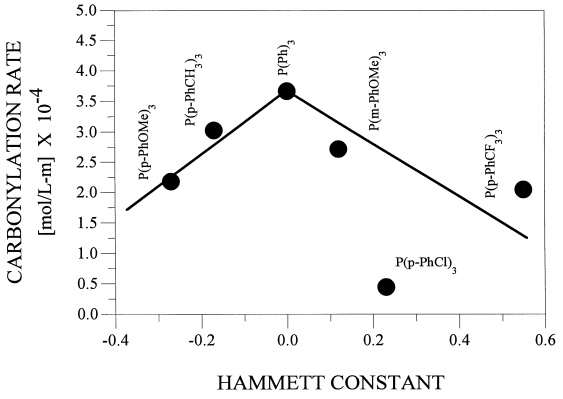

Fig. 5. Plot of the carbonylation rate as a function the electronic effects upon phosphorus as a measure of the normal Hammett sigma constant.

the sigma constants become more positive, it signifies increasing electron-withdrawing effects. Fig. 5 shows that the rate of acetic acid formation increased as the electron-donating ability of the groups to the left of *p*-H decreased (i.e., the Hammett constants increased from −0.3 towards 0.0). The carbonylation rate plot reached a maximum at PPh_3 where *p*-H is 0.0. Any further increase in the ligand's electron-withdrawing ability from sigma equal to 0.0 up to +0.60 served only to decrease the reaction rate. The observation of a volcano plot in Hammett treatments usually indicates a change in the rate-limiting step in a mechanism as the electronics are varied. One explanation for the reaction rate pattern is that as the electron donation from the ligand becomes very strong, the formation of the quaternary salt results in a stronger Me–P bond; therefore, less of the phosphine is available in an uncomplexed form. For the opposite case of strongly electron-withdrawing ligands, which do not strongly react with MeI, the coordinating ability of the free phosphines to nickel to form a species in the active cycle, $Ni(PR_3)_2$, is greatly reduced. Thus, the optimum ligand must have the best balance in its electronic character so that it has low reactivity toward MeI but strongly coordinates to Ni°.

Comparing the data presented in Figs. 3–5, relating the steric and electronic effects on the reaction rate, it can be seen that the highest rate of reaction was obtained when the steric size of the ligand was largest and electron donation was moderate (Fig. 3). When the electronic effects were isolated, it was found that they do play a role in the rate of reaction, as seen in Fig. 5, but the highest reaction rate was observed when the ligand was neither strongly electron-donating or -withdrawing. The overall highest MeOH carbonylation reaction rate was for the bulkiest ligand, P(*t*-butyl)$_3$, which has the highest cone angle and is also only moderately electron-donating.

4.5. Effect of free phosphine ligand concentration on carbonylation rate

To aid in understanding the effect of electronic variations in Figs. 4 and 5 on the carbonylation rate, the amount of free phosphine ligand was determined in the fast carbonylation rate regime in systems where the free phosphine could be reliably determined. Since P(*t*-butyl)$_3$ from the alkyl substitution series in Fig. 4 permitted reliable analysis of the amount of free phosphine, it was included in the study. Fig. 6 shows the results as a plot of carbonylation rate vs. free phosphine concentration in the fast rate regime after approximately 20% MeOH conver-

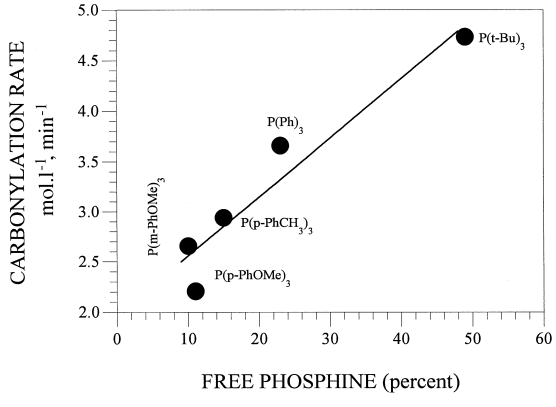

Fig. 6. The carbonylation reaction rate is plotted as a function of the percentage of the free phosphine as compared to the phosphonium salt after 20% MeOH conversion.

sion. The overall trend in the data indicates that the rate of reaction is dependent upon the ability of the phosphine promoter to provide an appropriate amount of free phosphine to the reaction mixture, that is not in the form of the corresponding phosphonium salt. We stress that the phosphine concentration determinations in these studies represent the total of PR_3 which is free (unbound in solution) plus the PR_3 which is coordinated to nickel. The infrared studies did not permit the separation of the PR_3 which is in solution and unbound to any other species from that which is bound to nickel, as $Ni(PR_3)_2$ or $Ni(PR_3)_n$ where $n = 1–4$. Hence, 'free phosphine' includes PR_3 in all species other than the phosphonium salts.

These findings are important in that they indicate that an important aspect of the promotion of the carbonylation rates by phosphines is the fine adjustment of the reacting components and process conditions so that all of the phosphine are not tied up as the phosphonium salt. The results of this study are in accord with the conclusions reached based on the in situ reaction-monitoring studies [14] while the process parameters were varied over a wide range. The results of the alkyl-substituted phosphines and *p*-substituted aryl phosphines agree with a mechanism in which a portion of the available nickel in the reactor is converted to Ni° which coordinates with the available free PR_3 to form $Ni(PR_3)_2$ which is within the active catalytic carbonylation cycle. The details of this mechanism will be discussed in a subsequent section.

Mizoroki and Nakayama [26–28] studied the visible and near ultraviolet spectra of cobalt iodide-catalyzed carbonylation of MeOH to MeOAc and hydrocarbonylation to form ethanol and concluded that most of the cobalt salts were tied up as $[CoI_n(OAc)_{(4-n)}]^{2-}$. An examination of the same catalyst system using phosphine ligands and an excess of methyl iodide by Gauthier-Lafaye and Perron [29] concluded that the applied phosphine was essentially converted irreversibly to the phosphonium iodide salt. Thus, they concluded that phosphine played no role in the active catalyst. The in situ studies reported here on similar systems containing high concentrations of phosphines and methyl iodide indicate that under reaction conditions, there is an observable dissociation of the quaternary phosphonium salt providing free phosphine to the catalytic system. Our data show that most of the phosphine originally applied was converted to the quaternary phosphonium salt through reaction with methyl iodide; however, under reaction conditions the back reaction was established. The degree of the back-reaction was dependent upon the temperature and structure of the phosphine. Based on the direct observation of free phosphines in the active solutions in this study and the similarity of the cobalt and nickel systems, it is likely that free phosphines were also present in the above mentioned cobalt catalyzed carbonylation systems and that phosphines may have been involved in the active catalytic cycle.

4.6. Role of $Ni(CO)_4$ on the reaction rate

In all of the carbonylation reactions, within the highest rate regime, either trace or large amounts of $Ni(CO)_4$ were present in the reactor depending on the structure of the phosphine promoter and the process parameters. In general, those conditions and promoters which resulted in high carbonylation rates resulted in trace concentrations of $Ni(CO)_4$. Fig. 7A shows a plot of the relative $Ni(CO)_4$ concentrations in solution in the reactor when several different trialkylphosphines were used as promoters. The $Ni(CO)_4$ concentration was measured in each experiment at the point of the highest rate. Fig. 7A also indicates the carbonylation rates observed when each of the phosphines was used as a promoter. The data in Fig. 7A show that the two promoters giving rise to the lowest reaction rates $P(CH_3)_3$, and $P(n\text{-}C_4H_9)_3$ displayed the highest concentration of $Ni(CO)_4$. The promoters resulting in the highest carbonylation rates like $P(i\text{-}C_3H_7)_3$, $P(C_6H_{11})_3$, and $P(t\text{-}C_4H_9)_3$ led to the lowest concentrations of $Ni(CO)_4$.

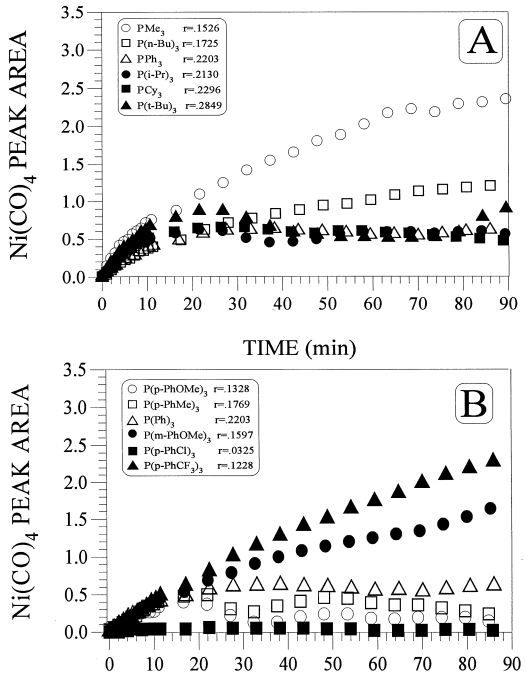

Fig. 7. The formation of $Ni(CO)_4$ is plotted as a function of reaction time for both series of reactions; Series (A) representing the alkyl groups: (○) Me; (□) *n*-butyl; (△) Ph_3; (●) *iso*-propyl; (■) cyclohexane; and (▲) *t*-butyl phosphines; and Series (B) for the substituted phenyl groups: (○) *para*-methoxyphenyl; (□) *para*-tolyl; (△) phenyl; (●) *meta*-methoxyphenyl; (■) *para*-chlorophenyl; and (▲) *para*-trifluoromethylphenyl phosphines.

The series involving the *p*-substituted aromatic phosphines generally show the same phenomenon. Measuring the $Ni(CO)_4$ concentration when various *p*-substituted arylphosphines were used in the carbonylation reaction showed that the reactions producing the most nickel carbonyl also resulted in the low reaction rates. These data are illustrated in Fig. 7B.

These experiments indicate two factors which regulate the amount of catalytically active species in solution under conditions of maximum rates. In the first case, when the nucleophilicity of the phosphorus atom is reduced by electron-withdrawing groups, it cannot successfully react with either MeI to form $[PMeR_3]^+I^-$ or Ni° in solution to form $Ni(PR_3)_2$. Both species are necessary for an active carbonylation system. On the other hand, if the nucleophilicity is high, as in the case using $P(CH_3)_3$, virtually all the PR_3 are taken out of solution by MeI, forming the corresponding phosphonium salt. In this case, there is little free PR_3 in solution to react with Ni° to form the active species in the cycle, $Ni(PR_3)_2$. Therefore, the optimal ligand would have electron-donating properties which are moderately strong to complex with Ni° in solution, and competing more strongly for the site than CO. The phosphine ligand must also be of the correct nucleophilicity to react with MeI, forming a phosphonium salt which is still able to dissociate the appropriate amount of free PR_3 to complex with Ni° to form a species within the catalytically active cycle, $Ni(PR_3)_2$.

The differences in the carbonylation reaction rate can be readily seen in comparing the various ligands in Table 4. For the alkyl-substituted phosphines, the highest rate was found for the bulkiest substituent (Fig. 3), which also had the smallest sigma* polarization contribution (Fig. 4). For the phenyl-substituted ligands, the highest carbonylation rate was for the unsubstituted PPh_3 molecule, the one with the neutral Hammett constant (Fig. 5).

5. Catalytic cycle

The overall mechanism that we propose is shown in Fig. 8. It is consistent with the in situ

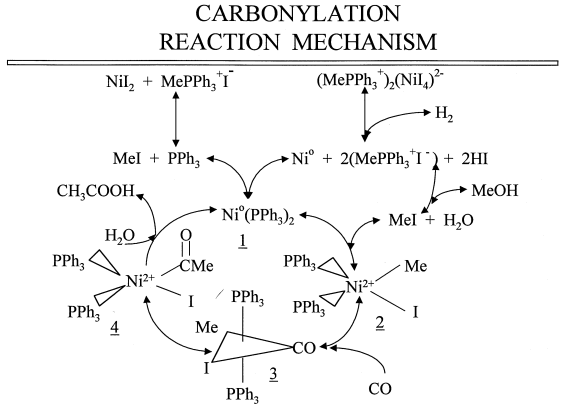

Fig. 8. Proposed mechanism for the nickel-catalyzed carbonylation on methanol to form acetic acid.

spectroscopic data and process parameter data described in our previous paper [14] as well as the ligand study presented in this paper. Although this study could not definitively specify the sequence of steps required to obtain Ni° in solution, it is clear that there must be a partial pressure of molecular hydrogen to start and maintain the carbonylation reaction. The principal evidence that Ni° is rapidly generated in the reactor is the observation that $Ni(CO)_4$ was observed in all cases, and its concentration was reduced by strongly coordinating ligands and enhanced by weakly coordinating ligands. Our in situ reaction-monitoring experiments showed that the pure phosphonium salt, $[PMePh_3]^+I^-$, partially dissociated to free phosphine under reaction conditions. Furthermore, the carbonylation rates were highest using those ligands where the concentration of free phosphine was highest when the infrared monitoring was conducted on the active systems. Thus, the optimum system contains sufficient free PR_3 to react with soluble Ni° in solution. The reduced Ni° may be in the form of $Ni(CO)_4$, or it may be immediately scavenged by PR_3 as soon as it is generated. The data do not permit us to distinguish between these two possibilities. Once the Ni° reacts with PR_3, it may form an active species such as $Ni(PR_3)_2$, or it can further react with PR_3 to form $Ni(PR_3)_3$ or $Ni(PR_3)_4$ which are likely inactive. Since our prior paper [14] showed that the carbonylation rate increased to a maxima followed by a decline as the P/Ni ratio increased, we take this as support for assigning the most active species as $Ni(PR_3)_2$. In addition, the very bulky ligand, $P(t\text{-}C_4H_9)_3$, gave the highest rate, and it would be expected to result in a coordination to Ni no greater than two PR_3/Ni. The next step in the cycle is the oxidative addition of methyl iodide to $Ni(PR_3)_2$, resulting in the four coordinate complex *2*. Our data [14] showed that the carbonylation rate was first-order with respect to methyl iodide concentration until the rate leveled-off at very high concentrations. A first order CH_3I dependence was also reported by Nelson et al. [12]. Our data also showed that the rate of carbonylation was first-order with respect to CO pressure. During the high carbonylation rate regime, no nickel carbonyl complexes could be detected by infrared monitoring except for traces of $Ni(CO)_4$. The infrared reaction-monitoring experiments did not permit one to distinguish between free PR_3, $Ni(PR_3)_n$, and the oxidative addition product *2*, $Ni(CH_3)(I)(PR_3)_2$. The combination of these facts leads to the conclusion that the reaction of methyl iodide with $Ni(PR_3)_2$ forms a low, equilibrium concentration of the four coordinate oxidative addition product *2* which is removed by reaction with CO. This aspect of the proposed mechanism is consistent with the observation of a first-order dependence on both methyl iodide and CO.

The subsequent steps in the catalytic cycle must be fast relative to the oxidative addition step since careful examination of the in situ reaction-monitored solutions showed no trace of a nickel carbonyl complex such as *3* or a nickel acetyl complex like *4*. The active catalytic cycle closely resembles the mechanism which we earlier proposed [30,31] for the phosphine-promoted palladium-catalyzed carbonylation of bromobenzene in MeOH to form methyl benzoate. Process conditions in the palladium study could be adjusted so that a $[PdBr(COR)L_2]$ complex could be observed in solution. The conversion of the acyl intermediate to methyl benzoate was shown to proceed via a direct reaction of MeOH rather than a reductive elimination forming the corresponding benzoyl bromide. Since the process conditions could not be adjusted in the present study to observe the acetyl complex *4* so that its reactivity could be determined, our data do not permit an assignment as to how the acetyl intermediate *4* further reacts to form acetic acid. Careful examination of the active solutions during conditions of high and low carbonylation rates did not result in the observation of any trace of acetyl iodide.

The generally accepted mechanism for this reaction proposed by Nelson et al. [12] consists of an active catalytic cycle containing only

nickel species containing a Ni–CO bond. The predominant intermediate observed under in situ reaction-monitoring conditions using transmission methods of infrared analysis was $[NiI(CO)_3]^-$. This intermediate is attractive since it is analogous to the predominant species, $[RhI_2(CO)_{22}]^-$, identified in the rhodium-catalyzed acetic acid process. However, the in situ reaction-monitoring studies based on CIR-FTIR used in the present study did not detect any of these species under conditions where the carbonylation rates were high. In addition, no nickel carbonyl (Ni–CO complex) of any kind could be detected, except for trace amounts of $Ni(CO)_4$. Had the Nelson-type mechanism been operative in the active solutions, we would have observed some Ni carbonyl complex. Since our active solutions contained no Ni carbonyl, and since the species observed are consistent with $Ni(PR_3)_2$ as the dominant Ni complex in solution, we conclude that the mechanism depicted in the active catalytic cycle in Fig. 8 is operative for this process.

Acknowledgements

The Department of Chemical Engineering of the Worcester Polytechnic Institute wishes to acknowledge a grant from Eastman Chemical to pursue this research. Also, acknowledgment is made to the National Science Foundation for a grant (CPE-8218110) which enabled the development of the CIR-reactor technology.

References

[1] F.E. Paulik, J.F. Roth, J. Chem. Soc., Chem. Commun. (1968) 1578.
[2] J.F. Roth, J.H. Craddock, A. Hershman, F.E. Paulik, Chem. Technol. (1971) 600.
[3] D.E. Morris, H.B. Tinker, Chem. Technol. (1972) 554.
[4] H.D. Grove, Hydrocarbon Proc. (1972) 76.
[5] D.J. Drury, M.J. Green, D.J.M. Ray, A.J. Stevenson, J. Organomet. Chem. 236 (1982) C23.
[6] T.W. Dekleva, D. Forster, J. Am. Chem. Soc. 107 (1985) 3565.
[7] W. Reppe, H. Friederich, N. von Kutepow, W. Morsch Badische Anilin- and Soda-Fabrik Aktiengesellschaft, U.S. Patent 2,729,651 (1956).
[8] F. Paulik, A. Hershman, J. Roth, Monsanto, U.S. Patent 3,769,329 (1973).
[9] D. Forster, T.C. Singleton, J. Mol. Catal. 17 (1982) 299.
[10] K. Fujimoto, K. Omata, T. Shikada, H. Tominaga, Homogeneous and heterogeneous catalysis, in: Yu. Yermakov, V. Likholobov (Eds.), VNU Science Press, Utrecht, the Netherlands (July 1986) p. 577.
[11] T.W. Dekleva, D. Forster, Adv. Catal. 34 (1986) 81.
[12] G.O. Nelson, E.C. Middlemas, S.W. Polichnowski, Presented to the New York Acad. Sci. (March 13, 1986).
[13] J. Gauthier-Lafaye, R. Perron, Methanol and Carbonylation, Technip edn., Rhône-Poulenc Recherches, Paris, France (1987) 117.
[14] W.R. Moser, B.J. Marshik-Guerts, S.J. Okrasinsky, J. Mol. Catal. A: Chem. 143 (1999) 57.
[15] W.R. Moser, J.E. Cnossen, A.W. Wang, S.A. Krouse, J. Catal. 95 (1985) 21.
[16] W.R. Moser, Homogeneous metal-catalyzed reactions, Adv. Chem. Ser. 230 (1992) 3.
[17] N. Rizkala, ACS Symp. Ser. 328 (1987) 61.
[18] A. Otsuka, S. Nakamura, Y. Yoshida, J. Am. Chem. Soc. 91 (1969) 7196.
[19] W. Reppe, N. von Kutepow, H. Bille, Badische Anilin- and Soda-Fabrik Aktiengesellschaft, U.S. Patent 3,014,962 (1961).
[20] W. Reppe, H. Kroper, N. von Kutepow, H. Pistor, Justus Liebigs Ann. Chem. 582 (1953) 72.
[21] J.R. Zoeller, private communication, Eastman Chemical, Kingsport TN, USA.
[22] C.A. Tolman, Chem. Rev. 77 (1977) 319.
[23] L.P. Hammett, Physical Organic Chemistry, McGraw-Hill, New York (1940) pp. 184–199.
[24] R.W. Taft, Steric effects in organic chemistry, in: M.S. Newman (Ed.), Wiley, New York, NY (1956) p. 619.
[25] T.H. Lowry, K.S. Richardson, Mechanism and Theory in Organic Chemistry, Harper Row Publishers (1980) p. 139.
[26] T. Mizoroki, M. Nakayama, Bull. Chem. Soc. (Japan) 38 (1965) 1876.
[27] T. Mizoroki, M. Nakayama, Bull. Chem. Soc. (Japan) 39 (1966) 1477.
[28] T. Mizoroki, M. Nakayama, Bull. Chem. Soc. (Japan) 41 (1968) 1628.
[29] J. Gauthier-Lafaye, R. Perron, Methanol and Carbonylation, Technip edn., Rhone-Poulenc Recherches, Paris, France (1987) p. 55.
[30] Moser, W.R., A.W. Wang, N.K. Kildahl, in: D.W. Blackburn (Ed.), Catal. Org. React., Vol. 137, Marcel Dekker, New York (1990).
[31] W.R. Moser, A.W. Wang, N.K. Kildahl, J. Am. Chem. Soc. 110 (1988) 2816.